Molecules and Cells

PRP4 Kinase Domain Loss Nullifies Drug Resistance and Epithelial-Mesenchymal Transition in Human Colorectal Carcinoma Cells

Muhammad Bilal Ahmed[1], Salman Ul Islam[1], Jong Kyung Sonn[2], and Young Sup Lee[1,*]

[1]School of Life Sciences, College of Natural Sciences, Kyungpook National University, Daegu 41566, Korea, [2]Department of Biology, College of Natural Sciences, Kyungpook National University, Daegu 41566, Korea
*Correspondence: yselee@knu.ac.kr
https://doi.org/10.14348/molcells.2020.2263
www.molcells.org

We have investigated the involvement of the pre-mRNA processing factor 4B (PRP4) kinase domain in mediating drug resistance. HCT116 cells were treated with curcumin, and apoptosis was assessed based on flow cytometry and the generation of reactive oxygen species (ROS). Cells were then transfected with PRP4 or pre-mRNA-processing-splicing factor 8 (PRP8), and drug resistance was analyzed both *in vitro* and *in vivo*. Furthermore, we deleted the kinase domain in PRP4 using Gateway™ technology. Curcumin induced cell death through the production of ROS and decreased the activation of survival signals, but PRP4 overexpression reversed the curcumin-induced oxidative stress and apoptosis. PRP8 failed to reverse the curcumin-induced apoptosis in the HCT116 colon cancer cell line. In xenograft mouse model experiments, curcumin effectively reduced tumour size whereas PRP4 conferred resistance to curcumin, which was evident from increasing tumour size, while PRP8 failed to regulate the curcumin action. PRP4 overexpression altered the morphology, rearranged the actin cytoskeleton, triggered epithelial-mesenchymal transition (EMT), and decreased the invasiveness of HCT116 cells. The loss of E-cadherin, a hallmark of EMT, was observed in HCT116 cells overexpressing PRP4. Moreover, we observed that the EMT-inducing potential of PRP4 was aborted after the deletion of its kinase domain. Collectively, our investigations suggest that the PRP4 kinase domain is responsible for promoting drug resistance to curcumin by inducing EMT. Further evaluation of PRP4-induced inhibition of cell death and PRP4 kinase domain interactions with various other proteins might lead to the development of novel approaches for overcoming drug resistance in patients with colon cancer.

Keywords: colorectal cancer, curcumin, EMT, HCT116, kinase domain, PRP4, PRP8

INTRODUCTION

PRP4 (pre-mRNA processing factor 4B), a transcription factor involved in pre-mRNA splicing, was first identified in *Schizosaccharomyces pombe* (Alahari et al., 1993; Rosenberg et al., 1991). It is 1,007 amino acids long and has been shown to possess a 340-amino acid Arg/Ser-rich N-terminal domain (RS domain) which is commonly found in pre-mRNA splicing factors (Haynes and Iakoucheva, 2006; Kojima et al., 2001). It has been reported that in addition to an RS domain, PRP4 contains a kinase domain (amino acid sequence 687-1003) which shares homology with cyclin-dependent kinases and mitogen-activated protein kinases (Kojima et al., 2001; Lützelberger and Käufer, 2012) and is essential for regulating cancer cell growth and survival (Gao et al., 2013). Previously, it has been reported that PRP4 is involved in reversing an-

Received 7 November, 2019; revised 23 April, 2020; accepted 26 April, 2020; published online 24 June, 2020

eISSN: 0219-1032

ticancer drug-induced cell death in human cancer cell lines through actin cytoskeleton rearrangement and epithelial-mesenchymal transition (EMT) (Islam et al., 2017; 2018). In attempts to determine kinases essential for pancreatic cancer cell survival using small-interfering RNAs (siRNAs), PRP4 knockdown was found to promote cell death and decrease viability (Giroux et al., 2006). Additionally, a study conducted to determine potential kinase targets to treat multidrug-resistant ovarian cancer showed that silencing PRP4 with short-hairpin RNAs (shRNAs) resulted in re-sensitization of chemo-resistant human ovarian cancer to paclitaxel (Duan et al., 2008). Moreover, it has been shown that PRP4 loss enhanced paclitaxel activity in breast cancer cells (Bauer et al., 2010).

EMT is a phenomenon in which epithelial cells lose cell-cell adhesion and transform into invasive mesenchymal cells (Du and Shim, 2016). During EMT, cells present reduced levels of epithelial proteins (E-cadherin, zonula occludens-1 [ZO-1], and occludin) and elevated levels of mesenchymal proteins (vimentin, N-cadherin, and fibronectin) (Lamouille et al., 2014). Loss of E-cadherin is considered a hallmark of EMT. Numerous phenotypic changes such as cell morphological changes, loss of adhesion, and gain of stem cell-like features have been reported upon changes in gene expression during EMT (Lamouille et al., 2014). The correlation between cancer cell drug resistance and EMT was first reported in a study in the early 1990s in which a vinblastine-resistant ZR-75-B cell line and two Adriamycin-resistant MCF-7 cell lines underwent EMT (Sommers et al., 1992). Recently, a causal relationship between EMT and cancer drug resistance using genetically-engineered mice models has been demonstrated by two research groups (Fischer et al., 2015; Zheng et al., 2015). In diverse cancers of the breast, bladder, and pancreas, cancer drug resistance has been shown to be frequently accompanied by EMT (Arumugam et al., 2009; Huang et al., 2015; McConkey et al., 2009). These reports suggest that EMT plays a key role in cancer drug resistance and contributes to metastasis after chemotherapy treatment.

Herein, we report that PRP4 mediates anti-apoptotic activities and induces resistance to the action of curcumin by driving HCT116 cells toward EMT. We supported our investigation by overexpressing pre-mRNA-processing-splicing factor 8 (PRP8) in HCT116 cells lines, which failed to reverse the action of curcumin. Finally, we produced kinase domain-deleted PRP4 ($P4K^{-/-}$) using Gateway™ technology, overexpressed it in HCT116 cells, and found that PRP4 lost its EMT-inducing potential upon kinase domain deletion. These findings advance our understanding of anticancer drug resistance in colon cancer.

MATERIALS AND METHODS

Chemicals and reagents

Curcumin and propidium iodide (PI) were purchased from Sigma-Aldrich (USA). Dulbecco's modified Eagle's medium (DMEM), fetal bovine serum (FBS), and penicillin/streptomycin were obtained from Gibco (USA). PRP4 cDNA open reading frame clone HG10835-ACG was purchased from Sino Biological (USA), and a PRP8 clone was obtained from Origene (USA). Antibodies against caspase-3, cleaved caspase-3, PARP (poly [ADP-ribose] polymerase), β-actin, Raf, p-Raf, Erk, p-Erk, NF-κB, IκB-α, p53, c-Myc, and Bcl-xL (B-cell lymphoma-extra-large) were obtained from Santa Cruz Biotechnology (USA). A Bradford protein assay kit and electrophoresis reagents were purchased from Bio-Rad (USA). Dichlorofluorescein diacetate (DCFHDA) was obtained from Molecular Probes (USA). ECL Prime detection reagent and nitrocellulose membrane were purchased from Amersham (UK). Vectashield mounting medium with DAPI (4′,6-diamidino-2-phenylindole) from Vector Laboratories (USA) was used for staining nuclei. An Annexin V-FITC apoptosis detection kit (ab14085 Abcam) was purchased from Abcam (UK). Lipofectamine® LTX with Plus™ Reagent (Cat. #15338100) and SuperScript III Reverse Transcriptase (Cat. #18080093), Lipofectamine RNAiMAX transfection reagent, and a pCR8-GW-TOPO TA cloning kit with One Shot™ TOP10 *E. coli* and the Gateway™ pDEST17 vector were obtained from Invitrogen (USA). Xfect transfection reagent was purchased from Takara Bio USA (USA). All chemicals and products were used as prescribed by the manufacturers.

Cell culture and treatment

HCT116 (CCL-225) cells from American Type Culture Collection (USA) were cultured in DMEM containing 10% FBS, L-glutamine, and 1% (v/v) penicillin-streptomycin (Gibco). Cells were maintained at 95% humidity with 5% CO_2 at 37°C. Curcumin was dissolved in dimethyl sulfoxide and cells were treated with 30 μM curcumin for 24 h (Shehzad et al., 2016).

Flow cytometry

HCT116 cells were cultured and treated with 30 μM curcumin for 24 h, after which they were washed twice with cold phosphate-buffered saline (PBS), trypsinized, centrifuged, and collected in 500 μl binding solution. Next, the cells were incubated with 5 μl each of Annexin V-FITC and PI (50 mg/ml) at room temperature for 15 to 20 min in the dark and analyzed by flow cytometry (FACSARIA III; BD Biosciences, USA) (Wlodkowic et al., 2009).

Detection of reactive oxygen species (ROS) generation

For the detection of intracellular ROS generation, cells were cultured in a 4-well plate at a density of 2×10^5 cells per well for 24 h. At 70% confluence, the cells were treated with curcumin for 24 h, after which the medium was replaced with fresh medium and the cells were incubated with the DCFHDA probe for 30 min, during which the DCFHDA was de-esterified and converted to highly fluorescent 2′, 7′-dichlorofluorescein upon oxidation. Afterward, the cells were washed twice with ice-cold PBS and images were captured with a confocal laser scanning platform (DM/R-TCS; Leica, Germany) coupled to a microscope (Leitz DM REB; Leitz, Germany) at excitation and emission wavelengths of 480 nm and 520 nm, respectively.

DAPI staining

Nuclear fragmentation was analyzed by staining apoptotic nuclei with DAPI. Cells were treated with curcumin for 24 h,

after which they were harvested, washed in cold PBS twice, and fixed with acetic acid:ethanol (1:3) for 15 min at room temperature. The fixed cells were then washed and stained with DAPI mounting solution for 15 min. Digital images were captured using a confocal microscope (Zeiss Axio Observer A1; Carl Zeiss, Germany) (Lee et al., 2018).

Western blotting

Total cell lysates were prepared using cell lysis buffer, and the protein concentration was determined using the Bio-Rad Protein Assay. Samples (20-40 μg) were prepared in sodium dodecyl sulfate (SDS) sample buffer, separated via 10% SDS-polyacrylamide gel electrophoresis, and transferred onto a nitrocellulose membrane. The membranes were blocked with 2% albumin (Gendept, USA) solution for 2 h at 4°C. Chemiluminescent signals were developed with Clarity™ ECL Western Blotting Substrate (Bio-Rad) according to the manufacturer's instructions.

Reverse-transcription polymerase chain reaction (RT-PCR)

Total RNA (5 μg) was reverse-transcribed using the SuperScript III First-strand synthesis kit, as has been described previously (Islam et al., 2015; 2018). The synthesized cDNA was incubated with RNase H at 37°C for 1 h. PCR was performed using 2 μl of cDNA and the following primers: Bcl-xL forward, 5′-GATCCCCATGGCAGCAGTAAAGCAAG-3′ and Bcl-xL reverse, 5′- CCCCATCCCGGAAGAGTTCATTCACT-3′; Bcl-2 forward, 5′GAGACAGCCAGGAGAAAT-3′ and Bcl-2 reverse, 5′-CCTGTGGATGACTGAGTA-3′; glyceraldehyde-3-phosphate dehydrogenase (GAPDH) forward, 5′-AGGGCTGCTTTTAACTCTGGT-3′ and GAPDH reverse, 5′-CCCCACTTGATTTTGGAGGGA-3′. PCR was performed under the following conditions: one cycle at 98°C for 3 min followed by 30 to 35 cycles at 95°C for 30 s, 55°C for 30 s, and 72°C for 30 s, with a final extension step at 72°C for 5 min. The amplified PCR products were analyzed via 2% agarose gel electrophoresis and EcoDye™ Nucleic Acid Staining Solution (Biofact, Korea); the relative intensities of the detected bands were measured on a Gel Doc2000 scanner (Bio-Rad).

In vivo xenograft tumors

Male BALB/c-n mice were purchased from Central Lab Animal (Korea) and were kept under conditions of a constant temperature of 22°C and a light/dark cycle of 12 h. Animal experimental protocols were approved by the Kyungpook National University Animal Care Committee. Six mice were kept in each group. At 6 weeks of age, each mouse was injected separately with the control and PRP4 or PRP8/ $P4K^{-/-}$-transfected HCT116 cells suspended in 150 μl PBS on separate sites (left and right) using sterile insulin syringes. One week after cell implantation, the mice were divided into two groups: (A) control (vehicle) and (B) curcumin (50 mg/kg intraperitoneal injection). Tumor volumes were recorded on a weekly basis using Vernier calipers, and calculated according to the formula: $V = 4/3\pi W2L$ (short size2 × long size/2) (mm^3). The tumors were then excised using scissors after 30 to 45 days (Ahn et al., 2017).

Cloning and construction of the kinase-domain$^{-/-}$ PRP4 plasmid

Gateway™ technology was used according to the manufacturer's instructions to delete the kinase domain (amino acid sequence 687-1003) from PRP4 and to make a new construct of it. First of all, *PRP4* without kinase domain was amplified using specific primers. PCR products were then cloned into the pCR8-GW-TOPO entry vector via the BP reaction. Cloned PCR products were sequence-checked (Macrogen, Korea) in the pCR8-GW-TOPO entry vector and were as predicted. For all cDNAs, five entry clones from individual bacterial colonies were subsequently used in LR reactions with the T7 promoter expression vector pDEST17 (Supplementary Fig. S1, Supplementary Table S1). Cloned PCR products were sequence-checked in the pDEST17 vector and were as predicted.

Boyden chamber cell invasion assay

HCT116 cell invasion was investigated using the Boyden Millipore chamber system. Briefly, inserts were incubated in serum-free medium for 2 to 3 h at room temperature to rehydrate the extracellular matrix layer. Afterward, cells were seeded onto the membrane of the upper chamber insert, placed in the wells of a 24-well plate containing 500 μl of full growth DMEM, and transfected with PRP4/$P4K^{-/-}$. After specific incubation periods, non-invading cells remaining on the upper surface of the membrane were removed with aseptic cotton swabs. For visualization, HCT116 cells that had invaded across the collagen to the lower surface of the membrane were stained with 5% Giemsa solution for 30 min at room temperature in the dark, after which they were washed with PBS, air-dried, and images of them were captured using a Nikon SMZ18 system (Bian et al., 2015).

Statistical analysis

All samples were prepared in triplicate and all experiments were repeated at least three times. Statistical analysis were performed through one way ANCOVA with Bonferroni-adjusted post hoc tests using IBM SPSS Statistics (ver. 25; IBM, USA). The data are presented as the mean ± SD. Differences between groups were evaluated with Student's *t*-tests. *P* values less than 0.05 were considered statistically significant.

RESULTS

PRP4 overexpression inhibits curcumin-induced cell death

To analyze the inhibitory role of PRP4 against curcumin-induced cell death, HCT116 cells were transiently transfected with PRP4 plasmid and then incubated with curcumin for 24 h. PRP4 overexpression was confirmed at the protein level via western blotting (Fig. 1A). For PRP4 knockdown, we used a pool of three target-specific siRNAs (PRP4-siRNA; 19-25 nucleotides in length) that downregulated PRP4 expression at the mRNA level (Fig. 1B). To investigate the effect of PRP4 on curcumin-induced ROS generation, cells were treated with curcumin and incubated with a specific cell-permeable fluorescent dye (DCFHDA). In curcumin-treated cells, a considerable increase in 2′, 7′-dichlorofluorescein fluorescence was observed and PRP4 overexpression prevented curcum-

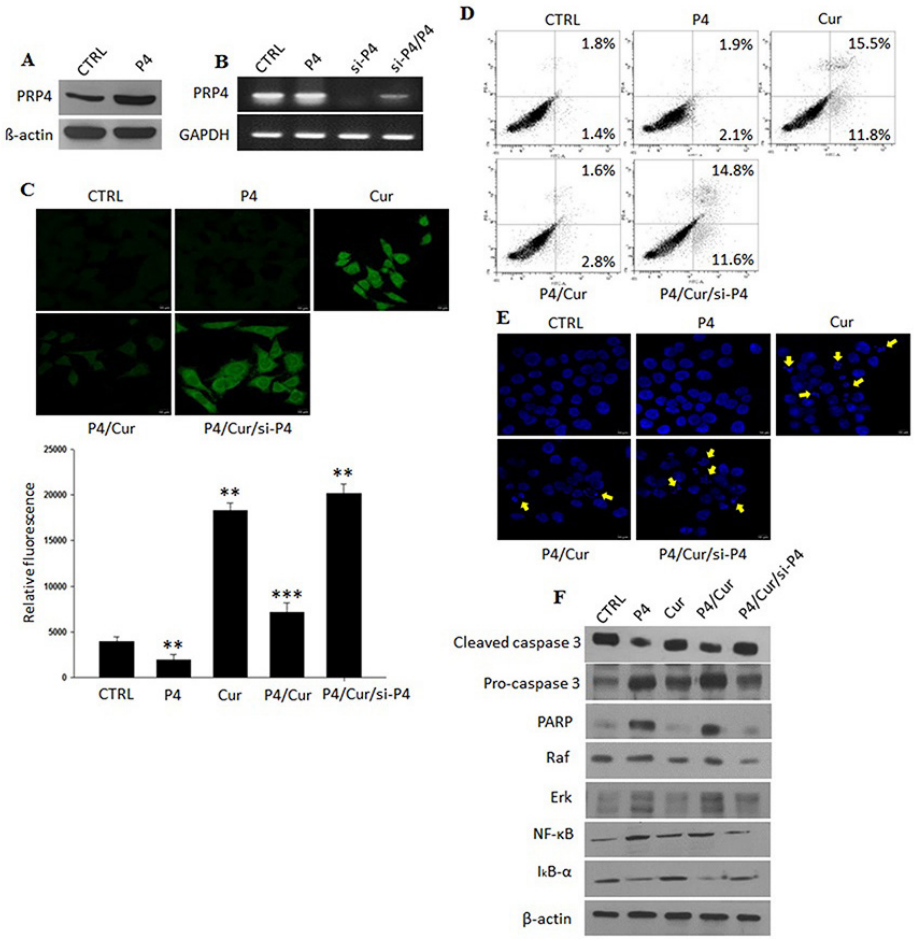

Fig. 1. PRP4 inhibited curcumin-induced cell death in HCT116 cells. (A) Western blot analysis of PRP4 overexpression in HCT116 cells. (B) PRP4 knockdown by siRNA PRP4 lowers the mRNA expression of PRP4 in HCT116 cells. GAPDH was used as a loading control. P4, PRP4 transfection; si-P4, siRNA PRP4 transfection. (C) HCT116 cells transfected with a PRP4 plasmid or siRNA-PRP4 and incubated with or without 30 μM curcumin for 24 h. The cells were incubated with the DCFHDA dye for 20 min to measure ROS. Probe accumulation was measured in triplicate based on increases in emission at a wavelength of 530 nm. ROS levels are expressed as the ratio of the mean intensity of the sample to the mean intensity in the control cells. The average fluorescence intensity was calculated and represented in graphical form. Data were collected from three independent experiments. $^{**}P < 0.01$, $^{***}P < 0.001$. (D) Parental and transfected HCT116 cells used in an Annexin V/propidium iodide (PI) assay and analyzed by flow cytometry to determine the levels of apoptosis. Upper left, necrotic cells; upper right, late apoptotic cells; lower right, early phase apoptotic cells; lower left, normal cells. (E) HCT116 cells transfected with a PRP4 plasmid or siRNA-PRP4 and incubated with or without 30 μM curcumin for 24 h. Cells were then stained with DAPI mounting solution for 20 min, washed twice with PBS, and analyzed via fluorescence microscopy. Yellow arrows represent fragmented nuclei. (F) Western blotting of parental and PRP4-transfected HCT116 cell lysates to assess cleaved caspase 3, pro-caspase 3, PARP, Raf, Erk, NF-κB, and IκB-α levels. β-actin was used as a loading control.

in-induced ROS generation (Fig. 1C), while PRP4-siRNA transfection restored curcumin-induced ROS generation (Fig. 1C). An Annexin V/PI apoptosis assay and flow cytometry were conducted to further address whether PRP4 inhibits curcumin-induced apoptosis. As depicted in Fig. 1D, curcumin treatment resulted in 11.8% and 15.5% of cells in early and late apoptosis, respectively, compared to untreated HCT116 cells (2% for each). PRP4 overexpression significantly reduced curcumin-induced apoptosis and brought the percentages of cells in early and late apoptosis to 2.8% and 1.6%, respectively (Fig. 1D). However, following concomitant transfection with a PRP4-expression plasmid and siRNA-PRP4, 11.6% of cells were observed in early apoptosis, which was close to the levels observed in curcumin-treated cells (Fig. 1D). Similar results were observed after staining the nuclei with DAPI (Fig. 1E). To further elucidate the anti-apoptotic effects of PRP4, we analyzed the changes in various cell death and survival regulatory proteins following PRP4 overexpression. Curcumin increased the expression of cleaved caspase 3, which was inhibited by PRP4 transfection. Similarly, we found that the 32 kDa caspase-3 zymogen as well as PARP had been restored following transfection with a PRP4-expressing plasmid in HCT116 cells, and similarly, PRP4 induced a number of cell survival signaling proteins (Fig. 1F). Collectively, these findings

suggest that PRP4 inhibits cell death in part by blocking the curcumin-induced generation of ROS and by activating cell survival pathways.

The kinase domain of PRP4 is involved in inhibiting curcumin-induced cell death

We hypothesized that PRP4 induces anti-apoptotic actions due to its kinase domain because it is the only member of the pre-mRNA splicing factor family which contains one. To prove this, we selected PRP8 (length = 2,335 amino acids), a homolog of PRP4 which lacks a kinase domain, and transfected HCT116 cells with a PRP8-expressing plasmid. PRP8 overexpression was confirmed at the protein level via western blotting (Fig. 2A). Subsequently, we repeated the assays outlined in Fig. 1 and found that PRP8 was not able to inhibit curcumin-induced apoptosis in HCT116 cells (Figs. 2B-2E). Bcl-xL and Bcl-2 are thought to exert an anti-apoptotic function (Michels et al., 2013), and the results in Fig. 2F show that curcumin downregulated their mRNA expression, but PRP8 overexpression could not restore it. Similarly, it was shown previously that PRP4 induced the expression of p53 (Shehzad et al., 2013), but PRP8 overexpression did not regulate it (Fig. 2E). We further conducted animal model xenograft assays to confirm the drug resistance potential and expressions of PRP4 and PRP8 *in vivo*. PRP4-transfected HCT116 cells showed remarkably enhanced expression and tumor growth compared with original HCT116 cells in the vehicle-treated group without affecting body weight (Fig. 3A). Additionally, as well as

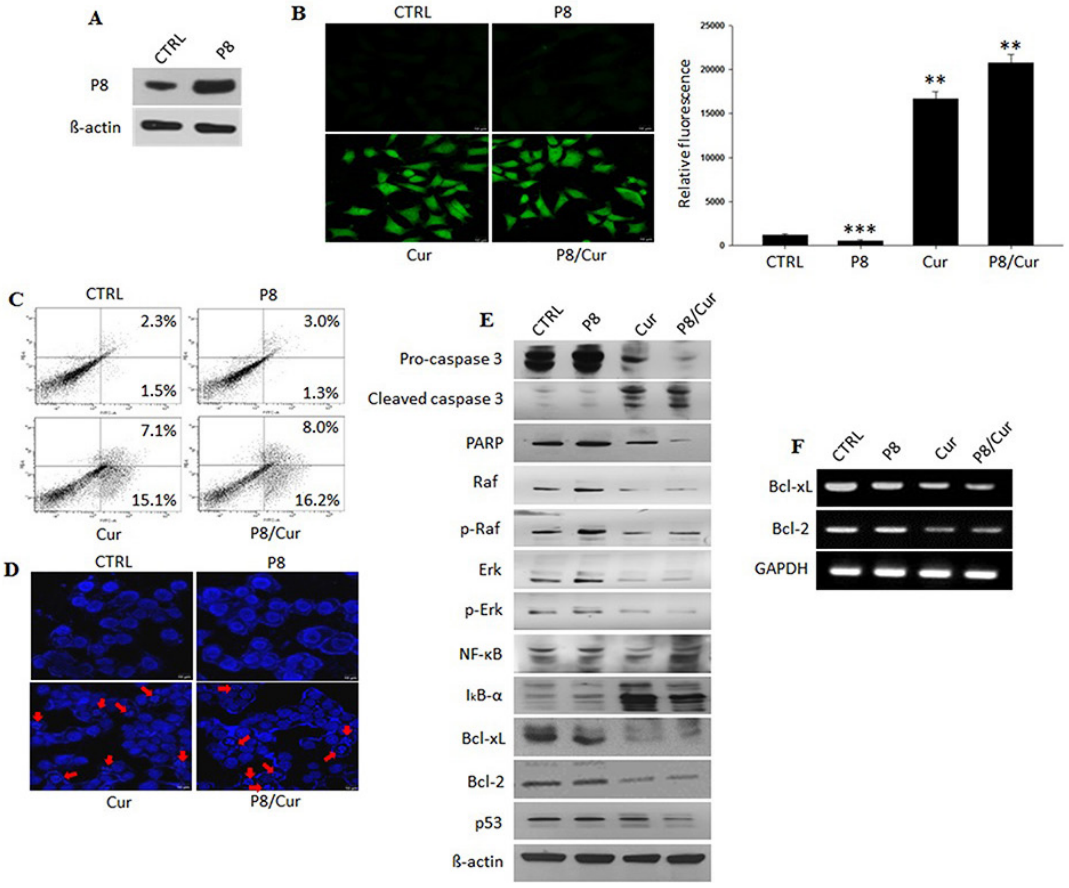

Fig. 2. PRP8 failed to reverse curcumin-induced cell death. (A) Western blot analysis of PRP8 overexpression in HCT116 cells. (B) HCT116 cells transfected with a PRP8 plasmid (P8, PRP8 transfection) and incubated with or without 30 μM curcumin for 24 h. The cells were incubated with the DCFHDA dye for 20 min to measure ROS. Probe accumulation was measured in triplicate based on increases in emission at a wavelength of 530 nm. ROS levels are expressed as the ratio of the mean intensity of the sample to the mean intensity in the control cells. The average fluorescence intensity was calculated and represented in graphical form. Data were collected from three independent experiments. $^{**}P < 0.01$, $^{***}P < 0.001$. (C) Parental and PRP8 transfected HCT116 cells followed by curcumin treatment in an Annexin V/propidium iodide (PI) assay was analyzed by flow cytometry to determine the levels of apoptosis. Upper left, necrotic cells; upper right, late apoptotic cells; lower right, early phase apoptotic cells; lower left, normal cells. (D) HCT116 cells transfected with a PRP8 plasmid and incubated with or without 30 μM curcumin for 24 h. Cells were then stained with DAPI mounting solution for 20 min, washed twice with PBS, and analyzed by fluorescence microscopy. Red arrows represent fragmented nuclei. (E) Western blotting of untransfected and PRP8-transfected HCT116 cell lysates to assess pro-caspase 3, cleaved caspase 3, PARP, Raf, p-Raf, Erk, p-Erk, NF-κB, IκB-α, Bcl-xL, Bcl-2, and p53 levels. β-actin was used as a loading control. (F) mRNA expression of Bcl-xL and Bcl-2. GAPDH was used as a loading control.

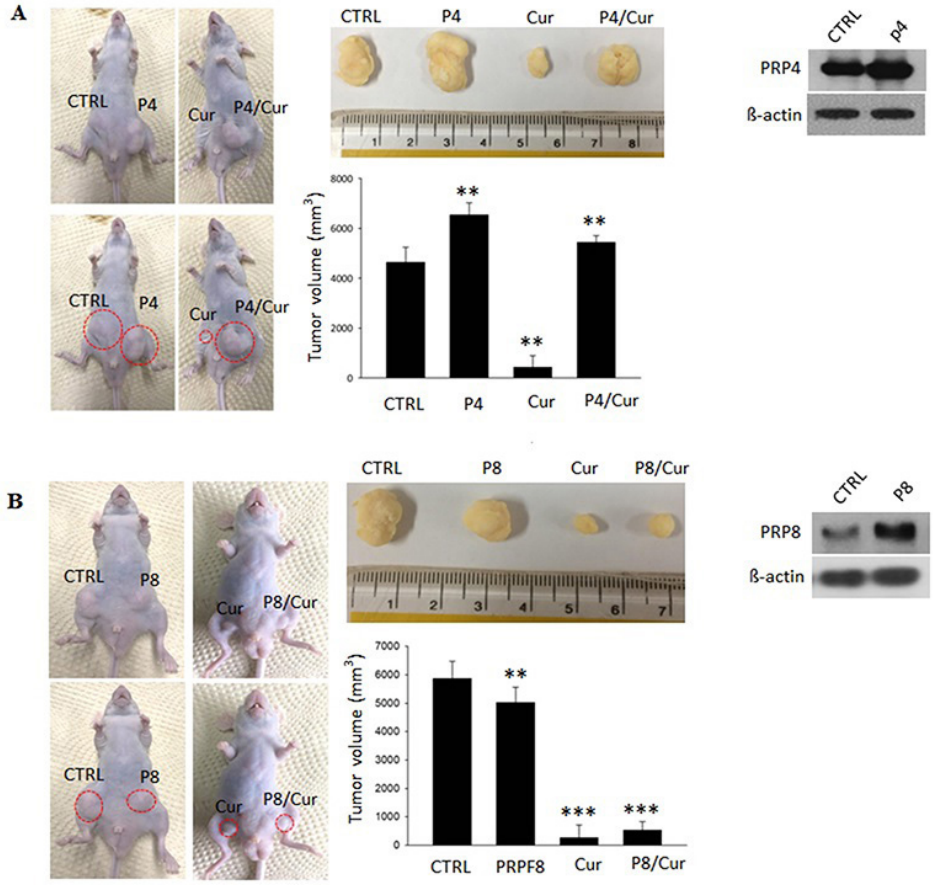

Fig. 3. PRP8 effect on xenograft tumors *in vivo*. (A) BALB/c-n mice were subcutaneously injected with HCT116 cells on the left side and with PRP4-transfected HCT116 cells on the right side (left and right sides are according to the photo). Six mice were kept in each group. Data were collected from three independent experiments. $**P < 0.01$. For clear visibility of the *in vivo* tumors, the same mouse was photographed twice and the tumors have been encircled in the later one. PRP4 overexpression has been shown in xenotransplant tumors through western blotting. (B) Same procedure was adopted as described above using PRP8-transfected HCT116 cells Data were collected from three independent experiments. $**P < 0.01$, $***P < 0.001$. PRP8 overexpression has been shown in xenotransplant tumors through western blotting.

conferring resistance to curcumin, PRP4-transfected HCT116 also showed enhanced tumor growth in the curcumin-treated group. Meanwhile, PRP8 shows increased expression but did not confer any remarkable resistance to curcumin, which was evident from the small tumor sizes compared to those observed in the curcumin-only group (Fig. 3B; tumor volume was measured according to the formula described in the Materials and Methods section and is presented as a line graph). These findings suggest that PRP4 confers resistance to curcumin-induced apoptosis *in vitro* as well as *in vivo* through its kinase domain.

Deletion of the PRP4 kinase domain aborts EMT

It has already been mentioned that cancer drug resistance is frequently accompanied by EMT (Arumugam et al., 2009; Huang et al., 2015; McConkey et al., 2009). To confirm that PRP4 conferred resistance to the action of curcumin by driving HCT116 cells toward EMT through its kinase domain, we completely removed it, as described in the Materials and Methods section (Supplementary Fig. S1, Supplementary Table S1). Figure 4A depicts the respective bands of the *PRP4* cDNA plasmid (9872 bp), *PRP4* full gene (3024 bp), and *PRP4* with the kinase domain deleted (2058 bp). We observed that besides preventing curcumin-induced cell death, *PRP4* overexpression changed the HCT116 cell morphology from an aggregated, flattened shape to a dispersed, round shape. However, interestingly, we observed that overexpression of HCT116 with $P4K^{-/-}$ did not induce cell morphology alteration (Fig. 4B). $P4K^{-/-}$ also did not induce tumor growth *in vivo* (Fig. 4C). It has been reported that the downregulation of intracellular adhesion molecules disrupts cell-cell adhesion, which is specific to EMT (Van Roy and Berx, 2008). The downregulation of E-cadherin is believed to be one of the most reliable markers of EMT (Acloque et al., 2009), and to investigate whether PRP4 induced EMT via the involvement of its kinase domain, we transfected HCT116 cells with PRP4 or the $P4K^{-/-}$-expression plasmid and analyzed E-cadherin protein levels by western blotting as well as immuno-

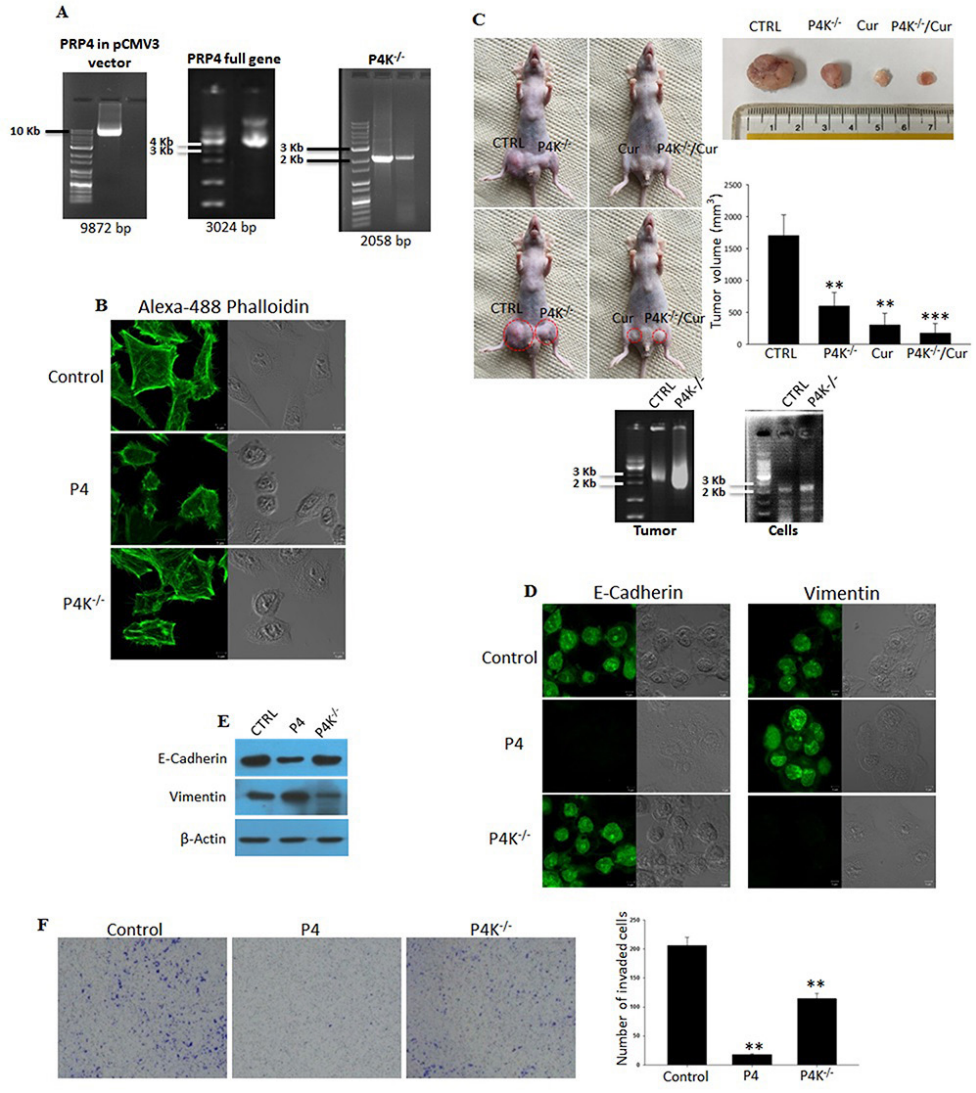

Fig. 4. PRP4 kinase domain deletion abolished the effect of PRP4 on cell cytoskeleton dynamics and EMT. (A) *PRP4* in the pCMV3 vector, *PRP4* full gene, and *PRP4* without a kinase domain in normal and Tumor cells. PRP4 was amplified using the specific primers given in Supplementary Table S1. (B) HCT116 cells transfected with a PRP4/P4K$^{-/-}$-expression plasmid, stained with phalloidin, and observed under a confocal laser microscope at 1,000× magnification. P4K$^{-/-}$, deleted PRP4 kinase-domain construct transfection. A grayscale image of the cells is also shown. (C) BALB/c-n mice were subcutaneously injected with HCT116 cells on the left side and with P4K$^{-/-}$-transfected HCT116 cells on the right side (left and right sides are according to the photo). Six mice were kept in each group. Data were collected from three independent experiments. $**P < 0.01$, $***P < 0.001$. For clear visibility of the *in vivo* tumors, the same mouse was photographed twice and the tumors have been encircled in the later one. P4K$^{-/-}$ overexpression has been shown on mRNA levels in xenotransplant tumors and cells. (D) Immunofluorescence microscopy indicating the expression of E-cadherin and vimentin following PRP4/P4K$^{-/-}$ overexpression in HCT116 cells shown by immunostaining with phalloidin, and E-cadherin and vimentin antibodies. A grayscale image of the cells is also shown. (E) E-cadherin, vimentin, and Tiam1 protein levels following PRP4/P4K$^{-/-}$ overexpression determined by western blotting. β-actin was used as an internal control. (F) Cellular invasion assay. The blue spots represent invaded cells. The average number of invaded cells have been shown in graphical form (n = 225, 23, and 125 in control, PRP4, and PRP4K$^{-/-}$ groups respectively, where n = number of invaded cells). $**P < 0.01$.

fluorescence. We found that PRP4 transfection effectively decreased E-cadherin expression in HCT116 cells but P4K$^{-/-}$ overexpression did not regulate E-cadherin expression. On the other hand, the mesenchymal marker vimentin showed upregulation upon PRP4 overexpression but remained unaffected by P4K$^{-/-}$ transfection (Figs. 4D and 4E). Cancer cells undergoing EMT display increased motility, acquire a mesenchymal phenotype, and subsequently become highly invasive (Micalizzi et al., 2010). To examine typical EMT behavior, we analyzed the cellular invasiveness of original and PRP4/P4K$^{-/-}$-

transfected HCT116 cells with a Boyden Millipore chamber system and observed that PRP4 transfection of HCT116 cells led to a remarkable decrease in cellular invasiveness. However, P4K$^{-/-}$ did not regulate cellular invasiveness (Fig. 4F). Collectively, these data suggest that PRP4 could induce EMT via the involvement of its kinase domain, thereby leading to resistance against curcumin-induced apoptosis.

DISCUSSION

The action of PRP4 in controlling cell growth in human cancer cells has been well described. Previously, it has been shown that PRP4 is involved in reversing anticancer drug-induced cell death in human cancer cell lines through actin cytoskeleton rearrangement and EMT (Islam et al., 2017; 2018). PRP4 has also been reported to induce the expression of protein phosphatase 1A (PP1A), which directly or indirectly dephosphorylates cofilin, resulting in actin cytoskeleton rearrangement, downregulation of E-cadherin, and EMT induction (Islam et al., 2018). In the present study, we observed that PRP4 reversed curcumin-induced apoptosis whereas siRNA-PRP4 transfection downregulated the expression of PRP4 and enhanced curcumin-induced apoptosis (Fig. 1). We were interested in investigating the involvement of the PRP4 kinase domain in mediating resistance to anticancer drugs, and structural approaches provided evidence that it was essential for regulating cancer cell growth and survival (Gao et al., 2013). For this purpose, we investigated various homologs of PRP4 lacking the kinase domain. Specifically, we selected PRP8 because unlike other PRP4 homologs, it possesses a protein length (2,335 amino acids) comparable to PRP4 (1,007 amino acids). Upon PRP8 transfection, we found that it did not block curcumin-induced apoptosis (Figs. 2B-2F). We further conducted animal model xenograft assays to confirm the action of PRP8 *in vivo*. Interestingly, the tumor generated by PRP8-transfected HCT116 cells did not grow more rapidly in mice in the control and curcumin-treated group, and curcumin effectively reduced the size of tumors resulting from implantation of the PRP8-transfected HCT116 cells (Fig. 3B). Cells were then transfected with P4K$^{-/-}$-expressing plasmid and their drug resistance potential was analyzed using various assays. As expected, P4K$^{-/-}$ failed to confer resistance to curcumin.

PRP4 overexpression induced morphological changes in HCT116 cells by rearranging the actin cytoskeleton and conferred resistance to curcumin-induced cell death. The findings from the present investigation suggest that resistance to curcumin-induced cell death conferred by PRP4 overexpression could be mediated through the modulation of the actin cytoskeleton and the PRP4 kinase domain is responsible for bringing about this morphological change. In original HCT116 cells, F-actin filaments were observed scattered throughout the entire cytoplasm in a pattern representative of the typical organization within migrating cells. However, in PRP4-transfected cells, confocal microscopy images showed that F-actin was distributed differently. We observed that P4K$^{-/-}$ overexpression could not alter the morphology of HCT116 cells. Studies have shown that the downregulation of intracellular adhesion molecules disrupts cell-cell adhesion specific to EMT, for which the downregulation of E-cadherin is a hallmark. We investigated the effect of PRP4 overexpression on E-cadherin protein expression by western blotting and immunostaining and found that PRP4 transfection effectively decreased E-cadherin expression in HCT116 cells. The expression of vimentin (a mesenchymal marker) was upregulated by PRP4 transfection but remained unaffected by P4K$^{-/-}$ overexpression. It has been shown that malignant cells undergoing EMT present increased motility, acquire the mesenchymal phenotype, and finally become highly invasive (Lamouille et al., 2014). We analyzed the cellular invasiveness of original and PRP4/P4K$^{-/-}$-transfected HCT116 cells and found that PRP4 transfection effectively decreased their cellular invasiveness whereas P4K$^{-/-}$ did not. These findings suggest that PRP4 could confer drug resistance to curcumin, partly by driving cancer cells toward EMT. We assume here that PRP4 through its kinase domain regulates the expression of EMT-associated genes in HCT116 cells to promote this transition. Furthermore, PRP4 regulates the expression of various other as yet unknown genes that are involved in increasing drug resistance and reducing cellular invasion.

In conclusion, collectively our study suggests that the PRP4 kinase domain is responsible for promoting drug resistance to curcumin and blocks apoptotic cell death by inhibiting curcumin-induced ROS generation, activating cell survival proteins, remodeling the cell actin cytoskeleton, and inducing EMT. Further evaluation of PRP4-induced anticancer drug resistance and PRP4 kinase domain interactions with various other proteins could lead to the development of novel approaches for overcoming drug resistance in patients with colon cancer. The determination of the direct and indirect target proteins of PRP4 and the exact molecular mechanism of activation or deactivation of these target proteins needs further intensive investigation.

Note: Supplementary information is available on the Molecules and Cells website (www.molcells.org).

ACKNOWLEDGMENTS
This research was supported by the National Research Foundation of Korea (NRF) grant funded by the Korean government (MSIT) (NRF-2019R1A2C1003003).

AUTHOR CONTRIBUTIONS
Y.S.L. and J.K.S. conceived and designed the experiments. M.B.A. and S.U.I. performed the experiments and wrote the manuscript.

CONFLICT OF INTEREST
The authors have no potential conflicts of interest to disclose.

ORCID
Muhammad Bilal Ahmed https://orcid.org/0000-0002-6816-4779
Salman Ul Islam https://orcid.org/0000-0001-6692-0270
Jong Kyung Sonn https://orcid.org/0000-0002-8200-9783
Young Sup Lee https://orcid.org/0000-0002-5841-6506

REFERENCES

Acloque, H., Adams, M.S., Fishwick, K., Bronner-Fraser, M., and Nieto, M.A. (2009). Epithelial-mesenchymal transitions: the importance of changing cell state in development and disease. J. Clin. Invest. *119,* 1438-1449.

Ahn, H.M., Yoo, J.W., Lee, S., Lee, H.J., Lee, H.S., and Lee, D.S. (2017). Peroxiredoxin 5 promotes the epithelial-mesenchymal transition in colon cancer. Biochem. Biophys. Res. Commun. *487,* 580-586.

Alahari, S.K., Schmidt, H., and Kaufer, N.F. (1993). The fission yeast prp4+ gene involved in pre-mRNA splicing codes for a predicted serine/threonine kinase and is essential for growth. Nucleic Acids Res. *21,* 4079-4083.

Arumugam, T., Ramachandran, V., Fournier, K.F., Wang, H., Marquis, L., Abbruzzese, J.L., Gallick, G.E., Logsdon, C.D., McConkey, D.J., and Choi, W. (2009). Epithelial to mesenchymal transition contributes to drug resistance in pancreatic cancer. Cancer Res. *69,* 5820-5828.

Bauer, J.A., Ye, F., Marshall, C.B., Lehmann, B.D., Pendleton, C.S., Shyr, Y., Arteaga, C.L., and Pietenpol, J.A. (2010). RNA interference (RNAi) screening approach identifies agents that enhance paclitaxel activity in breast cancer cells. Breast Cancer Res. *12,* R41.

Bian, Q., Liu, P., Gu, J., and Song, B. (2015). Tubeimoside-1 inhibits the growth and invasion of colorectal cancer cells through the Wnt/β-catenin signaling pathway. Int. J. Clin. Exp. Pathol. *8,* 12517.

Du, B. and Shim, J. (2016). Targeting epithelial-mesenchymal transition (EMT) to overcome drug resistance in cancer. Molecules *21,* 965.

Duan, Z., Weinstein, E.J., Ji, D., Ames, R.Y., Choy, E., Mankin, H., and Hornicek, F.J. (2008). Lentiviral short hairpin RNA screen of genes associated with multidrug resistance identifies PRP-4 as a new regulator of chemoresistance in human ovarian cancer. Mol. Cancer Ther. *7,* 2377-2385.

Fischer, K.R., Durrans, A., Lee, S., Sheng, J., Li, F., Wong, S.T., Choi, H., El Rayes, T., Ryu, S., and Troeger, J. (2015). Epithelial-to-mesenchymal transition is not required for lung metastasis but contributes to chemoresistance. Nature *527,* 472.

Gao, Q., Mechin, I., Kothari, N., Guo, Z., Deng, G., Haas, K., McManus, J., Hoffmann, D., Wang, A., Wiederschain, D., et al. (2013). Evaluation of cancer dependence and druggability of PRP4 kinase using cellular, biochemical, and structural approaches. J. Biol. Chem. *288,* 30125-30138.

Giroux, V., Iovanna, J., and Dagorn, J.C. (2006). Probing the human kinome for kinases involved in pancreatic cancer cell survival and gemcitabine resistance. FASEB J. *20,* 1982-1991.

Haynes, C. and Iakoucheva, L.M. (2006). Serine/arginine-rich splicing factors belong to a class of intrinsically disordered proteins. Nucleic Acids Res. *34,* 305-312.

Huang, J., Li, H., and Ren, G. (2015). Epithelial-mesenchymal transition and drug resistance in breast cancer. Int. J. Oncol. *47,* 840-848.

Islam, S.U., Ahmed, M.B., Lee, S.J., Shehzad, A., Sonn, J.K., Kwon, O.S., and Lee, Y.S. (2018). PRP4 kinase induces actin rearrangement and epithelial-mesenchymal transition through modulation of the actin-binding protein cofilin. Exp. Cell Res. *369,* 158-165.

Islam, S.U., Shehzad, A., and Lee, Y.S. (2015). Prostaglandin E2 inhibits resveratrol-induced apoptosis through activation of survival signaling pathways in HCT-15 cell lines. Anim. Cells Syst. (Seoul) *19,* 374-384.

Islam, S.U., Shehzad, A., Sonn, J.K., and Lee, Y.S. (2017). PRPF overexpression induces drug resistance through actin cytoskeleton rearrangement and epithelial-mesenchymal transition. Oncotarget *8,* 56659.

Kojima, T., Zama, T., Wada, K., Onogi, H., and Hagiwara, M. (2001). Cloning of human PRP4 reveals interaction with Clk1. J. Biol. Chem. *276,* 32247-32256.

Lamouille, S., Xu, J., and Derynck, R. (2014). Molecular mechanisms of epithelial-mesenchymal transition. Nat. Rev. Mol. Cell Biol. *15,* 178.

Lee, S., Lee, J.S., Seo, J., Lee, S.H., Kang, J.H., Song, J., and Kim, S.Y. (2018). Targeting mitochondrial oxidative phosphorylation abrogated irinotecan resistance in NSCLC. Sci. Rep. *8,* 15707.

Lützelberger, M. and Käufer, N.F. (2012). The Prp4 kinase: its substrates, function and regulation in pre-mRNA splicing. In Protein Phosphorylation in Human Health, C. Huang, ed. (London, UK: IntechOpen), Chapter 6.

McConkey, D.J., Choi, W., Marquis, L., Martin, F., Williams, M.B., Shah, J., Svatek, R., Das, A., Adam, L., and Kamat, A. (2009). Role of epithelial-to-mesenchymal transition (EMT) in drug sensitivity and metastasis in bladder cancer. Cancer Metastasis Rev. *28,* 335-344.

Micalizzi, D.S., Farabaugh, S.M., and Ford, H.L. (2010). Epithelial-mesenchymal transition in cancer: parallels between normal development and tumor progression. J. Mammary Gland Biol. Neoplasia *15,* 117-134.

Michels, J., Kepp, O., Senovilla, L., Lissa, D., Castedo, M., Kroemer, G., and Galluzzi, L. (2013). Functions of BCL-X L at the interface between cell death and metabolism. Int. J. Cell Biol. *2013,* 705294.

Rosenberg, G.H., Alahari, S.K., and Käufer, N.F. (1991). prp4 from Schizosaccharomyces pombe, a mutant deficient in pre-mRNA splicing isolated using genes containing artificial introns. Mol. Gen. Genet. *226,* 305-309.

Shehzad, A., Islam, S.U., Ahn, E.M., Lee, Y.M., and Lee, Y.S. (2016). Decursinol angelate inhibits PGE2-induced survival of the human leukemia HL-60 cell line via regulation of the EP2 receptor and NFkappaB pathway. Cancer Biol. Ther. *17,* 985-993.

Shehzad, A., Lee, J., Huh, T.L., and Lee, Y.S. (2013). Curcumin induces apoptosis in human colorectal carcinoma (HCT-15) cells by regulating expression of Prp4 and p53. Mol. Cells *35,* 526-532.

Sommers, C.L., Heckford, S.E., Skerker, J.M., Worland, P., Torri, J.A., Thompson, E.W., Byers, S.W., and Gelmann, E.P. (1992). Loss of epithelial markers and acquisition of vimentin expression in adriamycin-and vinblastine-resistant human breast cancer cell lines. Cancer Res. *52,* 5190-5197.

Van Roy, F. and Berx, G. (2008). The cell-cell adhesion molecule E-cadherin. Cell. Mol. Life Sci. *65,* 3756-3788.

Wlodkowic, D., Skommer, J., and Darzynkiewicz, Z. (2009). Flow cytometry-based apoptosis detection. Methods Mol. Biol. *559,* 19-32.

Zheng, X., Carstens, J.L., Kim, J., Scheible, M., Kaye, J., Sugimoto, H., Wu, C.C., LeBleu, V.S., and Kalluri, R. (2015). Epithelial-to-mesenchymal transition is dispensable for metastasis but induces chemoresistance in pancreatic cancer. Nature *527,* 525-530.